Songklanakarin J. Sci. Technol.
48 (2), e20260208, Mar. – Apr. 2026

http://www.sjst.psu.ac.th

Original Article

The effects of vaccination and mask-wearing on the mathematical model of influenza in Bangkok, Thailand

Jutarat Pholuang, and Nattakarn Numpanviwat*

Applied Mathematics Program, Faculty of Science and Technology,
Valaya Alongkorn Rajabhat University under the Royal Patronage,
Khlong Luang, Pathum Thani, 13180 Thailand

Received: 19 March 2025; Revised: 25 June 2025; Accepted: 30 October 2025

Abstract

Influenza (flu) is a contagious respiratory illness caused by influenza viruses. Bangkok, the densely populated capital of Thailand, had the second-highest illness rate for this disease. To better understand this situation, mathematical models have been developed and expressed through equations. This study presents a SEIRS compartmental model to investigate the transmission dynamics of influenza in Bangkok, with a particular focus on the impact of mask-wearing and vaccination interventions. The basic reproduction number was calculated using mathematical analysis, and the local stability of both disease-free and endemic equilibrium points was examined. Numerical simulations were conducted to assess how changes in transmission rates, mask-wearing, and vaccination coverage influence influenza outbreaks. The results indicate that higher transmission rates accelerate outbreak progression, whereas increased mask usage and vaccination rates substantially reduce disease spread. These findings highlight the critical role of public health measures, such as mask mandates and vaccination campaigns, in controlling influenza epidemics and minimizing their societal impact.

Keywords: influenza, mathematical model, vaccination, mask-wearing, stability analysis

1. Introduction

Influenza, commonly called the flu, is a contagious infection of the respiratory tract caused by influenza viruses. The illness typically begins suddenly and is marked by symptoms such as fever, cough, sore throat, nasal congestion, headaches, muscle or body aches, and pronounced fatigue (Centers for Disease Control and Prevention, 2024). Influenza virus primarily spreads through respiratory droplets released when an infected person coughs, sneezes, or talks, especially in crowded areas. Additionally, transmission can occur when a person touches surfaces contaminated with the virus and then touches their nose, mouth, or eyes, allowing the virus to enter the respiratory tract (Jan, 2024).

The incubation period lasts approximately 2 days. The patient is contagious starting 1 day before symptoms appear. Moreover, the appearance of symptoms has a spread of about 1 to 4 days. In most cases, fever and other symptoms typically resolve within 2 weeks or less without requiring medical treatment (Seladi-Schulman, 2023). Influenza can lead to severe illness or death, particularly in high-risk groups. These include individuals aged 65 years or older, pregnant women, children under 5 years old, people of any age with certain chronic medical conditions such as diabetes, asthma, or heart disease, and those with a body mass index (BMI) of 40 kg/m² or higher (Coleman, Fadel, Fitzpatrick, & Thomas, 2018).

Every year, seasonal influenza affects about one billion people globally, with 3 to 5 million cases developing into severe illness. This leads to approximately 290,000 to 650,000 deaths due to respiratory complications. In developing countries, 99 percent of deaths in children under five years old are caused by influenza-related lower respiratory tract infections (World Health Organization, 2025). It was reported

*Corresponding author
Email address: nattakarn.num@vru.ac.th

that in Thailand during 2024, there were 663,173 cases of influenza with 51 deaths recorded. The overall incidence rate was approximately 1,021.65 cases per 100,000 population. Children under 5 years old were identified as the highest risk group, with an incidence rate of 3,396.95 per 100,000 population, highlighting their vulnerability to influenza infection. Influenza A viruses have been identified as the main cause of the illness. In Bangkok, the incidence rate was recorded at 1,856.12 cases per 100,000 population, making it the second highest rate in Thailand for this disease (Division of Epidemiology, 2025).

Mathematical models have been developed and expressed through equations to better understand and represent the situation. These models have successfully predicted the behavior of the system (Tan, Yuan, Zhou, Zheng, & Yang, 2013; Viriyapong, 2021; Wu & Cowling, 2011). Many researchers have extensively studied the spread of influenza. Early modeling work concentrated on the Susceptible-Infected-Recovered (SIR) model, a basic framework that simplifies the process of disease spread by classifying individuals into separate categories (Furushima, Kawano, Ohno, & Kakehashi, 2017; Laguzet & Turinici, 2015; Safan, 2019). Although the SIR model laid an essential groundwork, its limitations - especially the assumption that immunity is permanent - revealed the necessity for more advanced and nuanced models.

The Susceptible-Exposed-Infected-Recovered (SEIR) model developed as a logical extension by adding an exposed category to represent the latent period typical of influenza (Alzahrani, Saadeh, Abdoon, Qazza, El Guma, & Berir, 2024; Imran, McKinney, & Butt, 2025). This improvement enabled a more accurate depiction of the disease's course, effectively modeling the crucial interval between becoming infected and becoming contagious. The SIRT and SEIRT models extend the traditional SIR and SEIR models by adding a new category, T, that usually denotes those who have been treated, quarantined, or placed in isolation (Maharany & Mardiningsih, 2022; Mohammad & Kamrujjaman, 2024). This modification helps better reflect public health strategies that emphasize isolating or controlling infectious cases to reduce disease transmission.

The decline of immunity over time and the appearance of new influenza strains led to the creation of the Susceptible-Exposed-Infected-Recovered-Susceptible(SEIRS) model (Amin, Majeed, Aziz, & Mustafa, 2024; Jia & Xiao, 2018). By allowing individuals to become susceptible again after recovery, the SEIRS model provides a more detailed perspective on the recurring patterns and long-term behavior of influenza. Additionally, recent research has expanded upon these foundational models by integrating elements such as co-infection dynamics and the effects of interventions like mask-wearing (Froese & Prempeh, 2022) and vaccination (Ho & Chao, 2020; Jonnalagadda, 2022), highlighting the continued importance of these modeling approaches in modern influenza studies.

Building on previous research, this study aims to develop a SEIRS model for influenza transmission in Bangkok, Thailand, that explicitly integrates the effects of both mask-wearing and vaccination. The objective is to analyze the model's stability characteristics by determining the basic reproduction number and examining the local stability of the disease-free and endemic equilibrium points. Furthermore, the study is numerically explored with regard to how varying transmission, mask-wearing and vaccination rates influence influenza dynamics. Through this comprehensive mathematical framework, the research intends to enhance understanding of how these interventions interact to control influenza outbreaks and to provide valuable insights for public health policy and the design of effective intervention strategies.

2. Materials and Methods

2.1 Formulation of the SEIRS model

In epidemiology, the SEIRS model mathematically describes the spread of influenza in Bangkok, incorporating factors with vaccination and mask-wearing. This model divides the population into four distinct groups that is susceptible (S), exposed (E), infected (I), and recovered (R). Figure 1 presents a block diagram of the SEIRS mathematical model of susceptible, exposed, infected, and recovered classes from the total population (N).

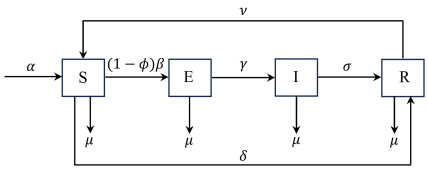

Figure 1. SEIRS mathematical model of influenza with mask-wearing and vaccination

As shown in Figure 1, the population is divided into four classes. S represents the susceptible group, consisting of individuals vulnerable to infection upon contact with the disease. E denotes the exposed group, which includes people who have been infected but are currently asymptomatic and not contagious. I stands for the infected group, comprising symptomatic patients who can transmit the disease. Lastly, R indicates the recovered group, made up of individuals who have recovered and possess temporary immunity.

In the SEIRS model, the coefficient α represents the birth rate, μ covers the death rate for susceptible, exposed, infected, and recovered classes, ϕ is the mask-wearing rate, δ indicates the vaccination rate, β corresponds to the transmission rate, γ captures the infected rate, σ describes the recovery rate, and ν reflects the rate at which immunity is lost. The mathematical representation of the SEIRS model is shown as a system of nonlinear ordinary differential equations which can be written as follows

$$\begin{aligned}
\frac{dS}{dt} &= \alpha N - \frac{(1-\phi)\beta SI}{N} + \nu R - \mu S - \delta S, \\
\frac{dE}{dt} &= \frac{(1-\phi)\beta SI}{N} - \gamma E - \mu E, \\
\frac{dI}{dt} &= \gamma E - \sigma I - \mu I, \\
\frac{dR}{dt} &= \sigma I - \nu R + \delta S - \mu R,
\end{aligned} \tag{1}$$

with initial conditions $S(0) = S_0 \geq 0$, $E(0) = E_0 \geq 0$, $I(0) = I_0 \geq 0$, and $R(0) = R_0 \geq 0$ for all time $t \geq 0$.

The total population is given by $N(t) = S(t) + E(t) + I(t) + R(t)$. When differentiating this equation with respect to time t, the resulting differential equation is

$$\frac{dN}{dt} = \frac{dS}{dt} + \frac{dE}{dt} + \frac{dI}{dt} + \frac{dR}{dt} = \alpha N - \mu(S + E + I + R) = (\alpha - \mu)N.$$

The solution to this linear differential equation is

$$N(t) = N_0 e^{(\alpha-\mu)t},$$

where $N_0 = N(0) = S(0) + E(0) + I(0) + R(0) > 0$ is the initial total population.

If $\alpha \leq \mu$, then $0 \leq N(t) \leq N_0$ for all $t \geq 0$. Since S, E, I, and R are non-negative and sum to N, it follows that S, E, I, and R are also bounded above by N_0.

If $\alpha > \mu$, then $N(t) \to \infty$ as $t \to \infty$. In this case $N(t)$ is unbounded. For the basic analysis presented here, we restrict our attention primarily to the case where $\alpha \leq \mu$, which prevents unbounded population growth.

2.2 Existence and positivity of solutions for the model

This section establishes the existence and positivity of solutions for the proposed system (1). The model parameters are assumed to be non-negative constants and the model is considered with non-negative initial conditions as stated in the previous section.

2.2.1 Existence and uniqueness of local solutions

The system of equations (1) can be rewritten using vector notation as the initial value problem

$$\frac{dX}{dt} = f(X), \qquad X(0) = X_0,$$

where $X = (S, E, I, R)^T$, $f: \mathbb{R}^4 \to \mathbb{R}^4$ is defined by the right-hand sides of the system (1), and $X_0 = (S_0, E_0, I_0, R_0)^T$. The function f is composed of polynomial and rational terms in the state variables S, E, I, R, and the total population N. On the domain $\Omega = \{X \in \mathbb{R}^4 : S \geq 0, E \geq 0, I \geq 0, R \geq 0 \text{ and } 0 \leq N \leq N_0\}$, f is continuous.

Furthermore, the partial derivatives of the component functions of f with respect to S, E, I, and R are bounded on any compact subset of Ω. Therefore, f is locally Lipschitz continuous on Ω. By the Picard–Lindelöf theorem (Coddington & Levinson, 1955), a unique solution $X(t)$ exists on some maximal interval of existence $[0, T_{max})$, where $T_{max} > 0$.

2.2.2 Positivity of solutions

To prove the positivity of the solutions, we need to analyze the equations and show that if the variables are non-negative at some time t, their derivatives will not force them to become negative at the next instant.

Firstly, consider the equation for dS/dt, assume $S(t) = 0$. Then

$$\frac{dS}{dt} = \alpha N + \nu R \geq 0,$$

since all parameters and variables on the right-hand side are non-negative. This means that if S reaches zero, it will not become negative.

Secondly, consider the equation for dE/dt, assume $E(t) = 0$. Then we obtain

$$\frac{dE}{dt} = \frac{(1-\phi)\beta SI}{N} \geq 0.$$

Again, if E reaches zero, it will not become negative.

Next, consider the equation for dI/dt, assume $I(t) = 0$. Then the equation becomes

$$\frac{dI}{dt} = \gamma E \geq 0.$$

Thus, I also remains non-negative.

Finally, consider the equation for dR/dt, assume $R(t) = 0$. Then we get

$$\frac{dR}{dt} = \sigma I + \delta S \geq 0.$$

So, R also remains non-negative.

In summary, we have shown that if any of the variables S, E, I, and R become zero, their derivatives are non-negative. This implies that these variables cannot become negative. Since the initial conditions S_0, E_0, I_0, and R_0 are assumed to be non-negative, the solutions $S(t)$, $E(t)$, $I(t)$, and $R(t)$ will remain non-negative for all $t \geq 0$.

2.3 Analysis of the SEIRS mathematical model

We analyze the system using the dimensionless variables $\bar{S} = \frac{S}{N}$, $\bar{E} = \frac{E}{N}$, $\bar{I} = \frac{I}{N}$, and $\bar{R} = \frac{R}{N}$. The resulting system of equations (see Appendix A for more details) is

$$\begin{aligned}
\frac{d\bar{S}}{dt} &= \alpha - (1-\phi)\beta\bar{S}\bar{I} + \nu\bar{R} - \alpha\bar{S} - \delta\bar{S}, \\
\frac{d\bar{E}}{dt} &= (1-\phi)\beta\bar{S}\bar{I} - \gamma\bar{E} - \alpha\bar{E}, \\
\frac{d\bar{I}}{dt} &= \gamma\bar{E} - \sigma\bar{I} - \alpha\bar{I}, \\
\frac{d\bar{R}}{dt} &= \sigma\bar{I} - \nu\bar{R} + \delta\bar{S} - \alpha\bar{R}.
\end{aligned} \tag{2}$$

Since $\bar{R} = 1 - \bar{S} - \bar{E} - \bar{I}$, the simplified model becomes

$$\begin{aligned}
\frac{d\bar{S}}{dt} &= (\nu + \alpha) - (1-\phi)\beta\bar{S}\bar{I} - \nu\bar{E} - \nu\bar{I} - (\nu + \alpha + \delta)\bar{S}, \\
\frac{d\bar{E}}{dt} &= (1-\phi)\beta\bar{S}\bar{I} - (\gamma + \alpha)\bar{E}, \\
\frac{d\bar{I}}{dt} &= \gamma\bar{E} - (\sigma + \alpha)\bar{I}.
\end{aligned} \tag{3}$$

The stability analysis will help us understand the long-term behavior of the system and the conditions under which the disease can be controlled or eradicated.

2.3.1 Equilibrium analysis

From the system of nonlinear ordinary differential equations (3), stability analysis has been carried out for the disease-free equilibrium (DFE) point, namely, $E_0 = (\bar{S}^0, \bar{E}^0, \bar{I}^0)$, and the endemic equilibrium (EE) point, namely, $E_1 = (\bar{S}^*, \bar{E}^*, \bar{I}^*)$. To determine the two equilibrium points, each equation in the system of equations (3) must be equal to zero, that is, $\frac{d\bar{S}}{dt} = 0$, $\frac{d\bar{E}}{dt} = 0$, and $\frac{d\bar{I}}{dt} = 0$, then

$$(\nu + \alpha) - (1 - \phi)\beta\bar{S}\bar{I} - \nu\bar{E} - \nu\bar{I} - (\nu + \alpha + \delta)\bar{S} = 0, \quad (4)$$

$$(1 - \phi)\beta\bar{S}\bar{I} - (\gamma + \alpha)\bar{E} = 0, \quad (5)$$

$$\gamma\bar{E} - (\sigma + \alpha)\bar{I} = 0. \quad (6)$$

1) Disease-free equilibrium

The DFE point is a condition with no influenza spread, then $\bar{E} = \bar{I} = 0$.

From equation (4), $(\nu + \alpha) - (\nu + \alpha + \delta)\bar{S} = 0$, we get $\bar{S}^0 = \frac{\nu+\alpha}{\nu+\alpha+\delta}$.

Therefore, the DFE point of the model is

$$E_0 = \left(\frac{\nu + \alpha}{\nu + \alpha + \delta}, 0, 0\right).$$

2) The basic reproduction number

The fundamental reproduction number of the model will be determined at the DFE point. This is the specific steady state of the epidemiological system where no infection persists in the population. Diekmann, Heesterbeek, and Metz (1990) established a foundational framework for calculating the basic reproduction number (R_0) in epidemiological models by introducing the next-generation matrix (NGM) method. This approach defines R_0 as the spectral radius (dominant eigenvalue) of the NGM. This matrix represents the expected number of secondary infections generated by individuals in different compartments. Van Den Driessche and Watmough (2002) formalized the NGM framework for compartmental models, providing a systematic decomposition of the Jacobian matrix into transmission and transition components. This work established the formula $R_0 = \rho(FV^{-1})$, where F and V are derived from transmission and transition components, and ρ denotes the spectral radius of the NGM.

Let $x = (S, E, I)^T$, the system (3) can be rewritten in the matrix form

$$\frac{dx}{dt} = \mathcal{F}(x) - \mathrm{V}(x),$$

where $\mathcal{F}(x) = \begin{pmatrix} 0 \\ (1 - \phi)\beta\bar{S}\bar{I} \\ 0 \end{pmatrix}$,

and

$$\mathrm{V}(x) = \begin{pmatrix} -(\nu + \alpha) + (1 - \phi)\beta\bar{S}\bar{I} + \nu\bar{E} + \nu\bar{I} + (\nu + \alpha + \delta)\bar{S} \\ (\gamma + \alpha)\bar{E} \\ -\gamma\bar{E} + (\sigma + \alpha)\bar{I} \end{pmatrix}.$$

Consider the disease classes (E and I compartment), the Jacobian matrices of $\mathcal{F}(x)$ and $\mathrm{V}(x)$ are evaluated as follows

$$F = \begin{pmatrix} 0 & (1 - \phi)\beta\bar{S} \\ 0 & 0 \end{pmatrix} \text{ and } V = \begin{pmatrix} \gamma + \alpha & 0 \\ -\gamma & \sigma + \alpha \end{pmatrix}.$$

Thus,

$$V^{-1} = \frac{1}{(\gamma+\alpha)(\sigma+\alpha)} \begin{pmatrix} \sigma + \alpha & 0 \\ \gamma & \gamma + \alpha \end{pmatrix} = \begin{pmatrix} \frac{1}{\gamma+\alpha} & 0 \\ \frac{\gamma}{(\gamma+\alpha)(\sigma+\alpha)} & \frac{1}{\sigma+\alpha} \end{pmatrix}.$$

Therefore, the NGM of the system (3) is

$$FV^{-1} = \begin{pmatrix} 0 & (1 - \phi)\beta\bar{S} \\ 0 & 0 \end{pmatrix} \begin{pmatrix} \frac{1}{\gamma+\alpha} & 0 \\ \frac{\gamma}{(\gamma+\alpha)(\sigma+\alpha)} & \frac{1}{\sigma+\alpha} \end{pmatrix} = \begin{pmatrix} \frac{(1-\phi)\beta\gamma\bar{S}}{(\gamma+\alpha)(\sigma+\alpha)} & \frac{(1-\phi)\beta\bar{S}}{\sigma+\alpha} \\ 0 & 0 \end{pmatrix}.$$

The basic reproduction number is defined as the spectral radius of the NGM. Hence, the spectral radius of FV^{-1} is

$$R_0 = \rho(FV^{-1}) = \frac{(1 - \phi)\beta\gamma\bar{S}}{(\gamma + \alpha)(\sigma + \alpha)}.$$

At the DFE point, we have derived $\bar{S} = \bar{S}^0 = \frac{\nu+\alpha}{\nu+\alpha+\delta}$. As a result, the basic reproduction number is

$$R_0 = \frac{(1 - \phi)\beta\gamma(\nu + \alpha)}{(\gamma + \alpha)(\sigma + \alpha)(\nu + \alpha + \delta)}.$$

3) Endemic equilibrium

The EE point is used to indicate the potential for disease transmission. Therefore, the population $\bar{S}^* \neq 0$, $\bar{E}^* \neq 0$, and $\bar{I}^* \neq 0$.

From equation (6), $\gamma\bar{E} - (\sigma + \alpha)\bar{I} = 0$, thus we get

$$\bar{E}^* = \left(\frac{\sigma + \alpha}{\gamma}\right)\bar{I}^*.$$

By substituting $\bar{E}^*$ into equation (5), we obtain the expression

$$\left[(1 - \phi)\beta\bar{S}^* - (\gamma + \alpha)\left(\frac{\sigma+\alpha}{\gamma}\right)\right]\bar{I}^* = 0.$$

Since $\bar{I}^* \neq 0$, we have the equation

$$(1 - \phi)\beta\bar{S}^* - (\gamma + \alpha)\left(\frac{\sigma+\alpha}{\gamma}\right) = 0.$$

Rearranging this equation, it follows that $\bar{S}^* = \frac{(\gamma+\alpha)(\sigma+\alpha)}{(1-\phi)\beta\gamma}$.

We can express $\bar{S}^*$ in terms of R_0 as

$$\bar{S}^* = \frac{\nu+\alpha}{(\nu+\alpha+\delta)R_0}.$$

Substituting $\bar{S}^*$ and $\bar{E}^*$ into equation (4) and simplifying yields

$$(\nu+\alpha) - \frac{(\gamma+\alpha)(\sigma+\alpha)}{\gamma}\bar{I}^* - \nu\left(\frac{\sigma+\alpha}{\gamma}\right)\bar{I}^* - \nu\bar{I}^* - \frac{\nu+\alpha}{R_0} = 0.$$

Rearranging this equation, we obtain

$$\bar{I}^* = \frac{\gamma(\nu+\alpha)(R_0-1)}{R_0[(\gamma+\alpha)(\sigma+\alpha)+\nu(\sigma+\alpha)+\nu\gamma]}.$$

Therefore, the EE point of the model is

$$E_1 = \begin{pmatrix} \frac{(\gamma+\alpha)(\sigma+\alpha)}{(1-\phi)\beta\gamma}, \left(\frac{\sigma+\alpha}{\gamma}\right)\bar{I}^*, \\ \frac{\gamma(\nu+\alpha)(R_0-1)}{R_0[(\gamma+\alpha)(\sigma+\alpha)+\nu(\sigma+\alpha)+\nu\gamma]} \end{pmatrix}.$$

2.3.2 Local stability analysis

To analyze the stability of the system, we evaluate the Jacobian matrix of system (3), which is

$$J = \begin{pmatrix} -(1-\phi)\beta\bar{I} - (\nu+\alpha+\delta) & -\nu & -(1-\phi)\beta\bar{S} - \nu \\ (1-\phi)\beta\bar{I} & -(\gamma+\alpha) & (1-\phi)\beta\bar{S} \\ 0 & \gamma & -(\sigma+\alpha) \end{pmatrix}. \quad (7)$$

1) Local stability of the DFE

For examining local stability, the Jacobian matrix corresponding to system (3) is evaluated at the DFE point. If $R_0 < 1$, then all eigenvalues of this Jacobian matrix have negative real parts. This implies that the DFE is locally asymptotically stable, meaning the disease will die out in the population near this equilibrium. On the other hand, if $R_0 > 1$, the DFE becomes unstable, and the system tends to the EE where disease persists in the population (Adom-Konadu, Sackitey, & Anokye, 2023).

Theorem 2.1 If $R_0 < 1$, the DFE is locally asymptotically stable; otherwise, if $R_0 > 1$, the DFE becomes unstable.

Proof. At the DFE point, by substituting $\bar{S} = \bar{S}^0 = \frac{(\gamma+\alpha)(\sigma+\alpha)R_0}{(1-\phi)\beta\gamma}$ and $\bar{I} = \bar{I}^0 = 0$ into equation (7), we derive

$$J_0 = \begin{pmatrix} -(\nu+\alpha+\delta) & -\nu & -\frac{(\gamma+\alpha)(\sigma+\alpha)R_0}{\gamma} - \nu \\ 0 & -(\gamma+\alpha) & \frac{(\gamma+\alpha)(\sigma+\alpha)R_0}{\gamma} \\ 0 & \gamma & -(\sigma+\alpha) \end{pmatrix}.$$

The eigenvalues are determined by solving the characteristic equation given by $\det(J_0 - \lambda I) = 0$, where λ represents the eigenvalues and I is the identity matrix.

The computation yields one eigenvalue as $\lambda_1 = -(\nu+\alpha+\delta) < 0$. The other two eigenvalues satisfy the quadratic equation

$$\lambda^2 + A\lambda + B = 0, \quad (8)$$

with $A = (\gamma+\alpha) + (\sigma+\alpha)$ and $B = (\gamma+\alpha)(\sigma+\alpha)(1-R_0)$.

When $R_0 < 1$, it follows that both $A > 0$ and $B > 0$. By the Routh-Hurwitz criterion (Bodson, 2019), all eigenvalues of equation (8) have negative real parts.

Therefore, the DFE is locally asymptotically stable.

If $R_0 > 1$, then $A > 0$, and $B < 0$. According to the Routh-Hurwitz criterion, this implies that equation (8) has at least one eigenvalue with a positive real part.

Therefore, the DFE is unstable. □

2) Local stability of the EE

Local stability analysis involves evaluating the Jacobian matrix associated with system (3) at the EE point. If $R_0 > 1$, all eigenvalues of this Jacobian matrix have negative real parts. This implies that the EE is locally asymptotically stable, indicating the disease remains endemic in the population. Conversely, if $R_0 < 1$, the EE becomes unstable, causing the system to move toward a state where the disease no longer persists (Adom-Konadu *et al*., 2023).

Theorem 2.2 If $R_0 > 1$, the EE is locally asymptotically stable; conversely, if $R_0 < 1$, the EE becomes unstable.

Proof. At the EE point, by substituting $\bar{S} = \bar{S}^* = \frac{(\gamma+\alpha)(\sigma+\alpha)}{(1-\phi)\beta\gamma}$ and $\bar{I} = \bar{I}^* = \frac{\gamma(\nu+\alpha)(R_0-1)}{R_0[(\gamma+\alpha)(\sigma+\alpha)+\nu(\sigma+\alpha)+\gamma\nu]}$ into equation (7), we obtain the Jacobian matrix

$$J_1 = \begin{pmatrix} -a_4(R_0-1) - a_3 & -\nu & -\frac{a_1a_2}{\gamma} - \nu \\ a_4(R_0-1) & -a_1 & \frac{a_1a_2}{\gamma} \\ 0 & \gamma & -a_2 \end{pmatrix},$$

where the parameters are defined as $a_1 = \gamma+\alpha$, $a_2 = \sigma+\alpha$, $a_3 = \nu+\alpha+\delta$, and $a_4 = \frac{a_1a_2a_3}{a_1a_2+a_2\nu+\gamma\nu}$.

The eigenvalues are found by solving the characteristic equation, which is given by $\det(J_1 - \lambda I) = 0$.

The characteristic equation can be expressed as

$$\lambda^3 + A\lambda^2 + B\lambda + C = 0, \quad (9)$$

where the coefficients are defined as

$$A = a_1 + a_2 + a_3 + a_4(R_0-1),$$
$$B = (a_1+a_2)a_3 + (a_1+a_2+\nu)a_4(R_0-1),$$
and $$C = a_1a_2a_3(R_0-1).$$

When $R_0 > 1$, it follows that $A, B, C > 0$, and $AB > C$ (see Appendix B for more details). By the Routh-Hurwitz criterion (Bodson, 2019), all eigenvalues of equation (9) have negative real parts.

Therefore, the EE is locally asymptotically stable.

If $R_0 < 1$, then $A < 0$, $B < 0$, and $C < 0$. According to the Routh-Hurwitz criterion, this implies that equation (9) has at least one eigenvalue with a positive real part.

Therefore, the EE is unstable. □

3. Results and Discussion

In this section, we present numerical simulations of the SEIRS model (system (2)) to illustrate the impact of key epidemiological parameters on influenza dynamics. Specifically, we investigate the influence of the transmission rate, mask-wearing rate, and vaccination rate on the spread of influenza within a population.

The parameters used in the model are estimated based on literature reviews and represent typical ranges for influenza dynamics. Abbasi, Zamani, Mehra, Ibeas, and Shafieirad (2021) employed a time-dependent transmission rate (β), varying between 0.5 and 2 to reflect contact rates in day and night. The inverse of the infected rate (γ) and the recovery rate (σ) represent the average latent period and the average recovery period, respectively. The latent period of 2 days ($1/\gamma$) is a common assumption in influenza modeling and the recovery period for influenza is typically around 2 weeks ($1/\sigma$) (Seladi-Schulman, 2023). The loss of immunity rate (ν) is often around 1/365 per day, reflecting the need for annual vaccination due to waning immunity and viral evolution (Armitage, 2024). The remaining parameters are estimated using clinical data, public health surveys, vital statistics, or demographic data. Details of all parameter values are provided in Table 1.

Figure 2 presents the variation in the proportion of individuals in each compartment of the SEIRS model over time, specifically when the transmission rate (β) is 0.5, with the initial conditions of $(\bar{S}_0, \bar{E}_0, \bar{I}_0, \bar{R}_0) = (0.99, 0.00, 0.01, 0.00)$. The simulation shows a rapid decline in susceptible individuals as they become exposed, followed by a quick rise and fall in exposed individuals. The proportion of infected individuals rises sharply to a peak before declining to a low, stable level, while recovered individuals increase rapidly and reach a high, stable level, indicating a sharp epidemic peak that eventually stabilizes with a large proportion of the population recovering and a small proportion remaining susceptible and infected.

Figures 3 and 4 illustrate the impact of varying the transmission rate (β) on the proportion of individuals in the infected ($\bar{I}$) and recovered ($\bar{R}$) classes over time, respectively. The plots compare the dynamics of the infected and recovered populations for four different values of β: 0.5, 1.0, 1.5, and 2.0. As shown in the figures, higher values of β lead to a larger and earlier peak in the proportion of infected individuals. This indicates that a higher transmission rate results in a more rapid and widespread outbreak. After the initial peak, the proportion of infected individuals declines over time for all values of β; however, the rate of decline and the final level of infected individuals vary depending on β, with higher values of β resulting in a slower decline and a higher endemic level of infection. Similarly, the proportion of recovered individuals increases over time for all values of β, and higher values of β lead to a more rapid increase in the proportion of recovered individuals. This is because a higher transmission rate results in a larger number of individuals becoming infected and subsequently recovering.

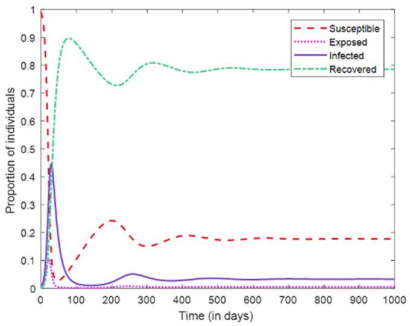

Figure 2. Compartmental dynamics of the SEIRS model with the transmission rate (β) fixed at 0.5

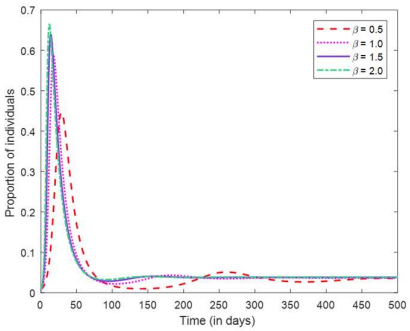

Figure 3. Impact of transmission rate (β) on infected class ($\bar{I}$)

Table 1. Parameters used in the investigation

Parameter	Symbol	Value	Unit	Source
Birth rate	α	2.615×10^{-5}	per day	BORA (2024)
Vaccination rate	δ	1.831×10^{-4}	per day	DDC (2024)
Mask-wearing rate	ϕ	0.194	per day	Leowattana (2025)
Transmission rate	β	$0.5 - 2.0$	per day	Abbasi *et al*. (2021)
Infected rate	γ	0.5	per day	Seladi-Schulman (2023)
Recovery rate	σ	0.071	per day	Seladi-Schulman (2023)
Loss of immunity rate	ν	0.003	per day	Armitage (2024)

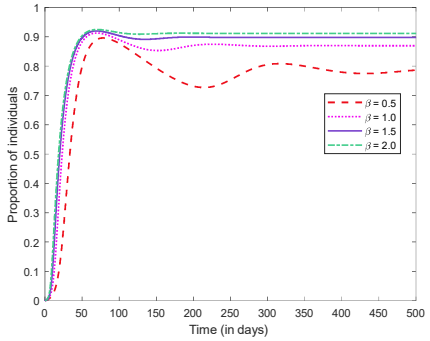

Figure 4. Impact of transmission rate (β) on recovered class ($\bar{R}$)

Figures 5 and 6 demonstrate the impact of varying the mask-wearing rate (ϕ) on the proportion of infected and recovered individuals over time, with the transmission rate (β) fixed at 0.5. The plot of infected individuals compares the dynamics of the infected population for five different values of ϕ: 0.2, 0.4, 0.6, and 0.8. As shown, increasing ϕ significantly reduces both the peak proportion of infected individuals and delays the timing of the peak. This indicates that higher mask-wearing rates can effectively mitigate and slow down the spread of the influenza virus. Additionally, higher ϕ values lead to a lower endemic level of infection. The plot of recovered individuals shows that the proportion of recovered individuals increases over time for all values of ϕ. The rate at which the recovered proportion approaches its maximum, and the final proportion of recovered individuals, both vary with ϕ. Specifically, higher mask-wearing rates (ϕ) lead to a slightly slower increase in the proportion of recovered individuals, as higher ϕ values lead to fewer infections, and recovery only occurs following infection.

Figures 7 and 8 show how changing the vaccination rate (δ) affects the number of infected and recovered people over time, assuming the transmission rate (β) is 0.5. The plot of infected individuals compares how the infected population changes for four different vaccination rates (δ): $10^{-4}, 10^{-3}, 10^{-2}$, and 10^{-1}. The figure shows that when the vaccination rate (δ) increases, the proportion of infected individuals decreases over time, and the peak of the infection is lower. This means that higher vaccination rates help to reduce and slow down the spread of the flu. Also, higher δ values lead to a lower endemic level of infection. The plot of recovered

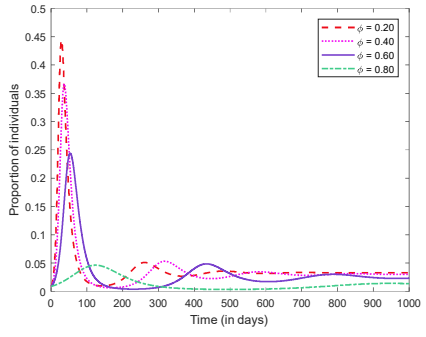

Figure 5. Impact of mask-wearing rate (ϕ) on infected class ($\bar{I}$) with the transmission rate (β) fixed at 0.5

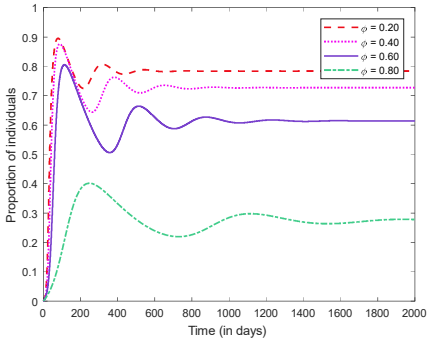

Figure 6. Impact of mask-wearing rate (ϕ) on recovered class ($\bar{R}$) with the transmission rate (β) fixed at 0.5

individuals shows that as the vaccination rate (δ) increases, the proportion of recovered individuals increases over time. Higher vaccination rates cause a more rapid increase in the proportion of recovered individuals.

Our numerical simulations demonstrate the significant impact of transmission rate (β), mask-wearing rate (ϕ), and vaccination rate (δ) on influenza dynamics. Higher transmission rates lead to larger and more rapid outbreaks, while increased mask-wearing and vaccination rates can effectively reduce the spread of influenza. These findings underscore the importance of public health interventions, such as mask mandates and vaccination campaigns, in mitigating the impact of influenza epidemics.

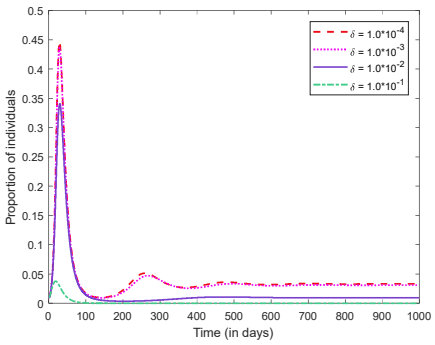

Figure 7. Impact of vaccination rate (δ) on infected class ($\bar{I}$) with the transmission rate (β) fixed at 0.5

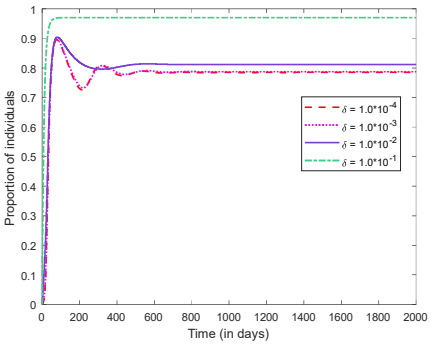

Figure 8. Impact of vaccination rate (δ) on recovered class ($\bar{R}$) with the transmitssion rate (β) fixed at 0.5

4. Conclusions

This study developed a SEIRS model to describe influenza transmission dynamics in Bangkok, Thailand, explicitly incorporating the effects of both mask-wearing and vaccination interventions. Through mathematical analysis, we determined the basic reproduction number and examined the local stability of both disease-free and endemic equilibrium points. Numerical simulations further explored how variations in transmission, mask-wearing, and vaccination rates affect influenza dynamics. The numerical simulations illustrated that higher transmission rates led to larger and more rapid outbreaks, while increased mask-wearing and vaccination rates can effectively reduce the spread of influenza.

Our findings are consistent with previous research, such as the study by Froese and Prempeh (2022), and Jonnalagadda (2022), which also demonstrated that widespread mask usage and vaccination campaigns significantly decrease influenza transmission within communities. These findings underscore the importance of public health interventions, such as mask mandates and vaccination campaigns, in mitigating the impact of influenza epidemics. Furthermore, this modeling framework can be adapted for use in other urban environments or for different respiratory infectious diseases by adjusting key parameters to reflect local epidemiological and behavioral characteristics.

Author Contributions

Jutarat Pholuang: Conceptualization, Investigation, Data curation, Writing - Original draft. Nattakarn Numpanviwat: Methodology, Software, Visualization, Validation, Writing - Reviewing and Editing.

References

Abbasi, Z., Zamani, I., Mehra, A. H. A., Ibeas, A., & Shafieirad, M. (2021). Optimal allocation of vaccine and antiviral drugs for influenza containment over delayed multiscale epidemic model considering time-dependent transmission rate. *Computational and Mathematical Methods in Medicine*, *2021*, 1–27. doi:10.1155/2021/4348910

Adom-Konadu, A., Sackitey, A. L., & Anokye, M. (2023). Local stability analysis of epidemic models using a corollary of Gershgorin's circle theorem. *Applied Mathematics E-Notes*, *23*, 159-174.

Alzahrani, S. M., Saadeh, R., Abdoon, M. A., Qazza, A., El Guma, F., & Berir, M. (2024). Numerical simulation of an influenza epidemic: prediction with fractional SEIR and the ARIMA model. *Applied Mathematics and Information Sciences, 18*(1), 1-12. doi:10.18576/amis/180101

Amin, S., Majeed, S., Aziz, S., & Mustafa, A. (2024). Bifurcation and global stability of a SEIRS model with a modified nonlinear incidence rate. *Journal of Applied Mathematics*, *2024*, 6253301. doi:10.1155/jama/6253301

Armitage, M. (2024). Flu vaccines. Retrieved from https://www.goodrx.com/conditions/flu-vaccination

Bodson, M. (2019). Explaining the Routh-Hurwitz criterion. Retrieved from https://my.eng.utah.edu/~bodson/pdf/Explaining%20the%20Routh-Hurwitz%20Criterion%20A%20Tutorial%20Presentation.pdf

Bureau of Registration Administration (BORA). (2024). Monthly statistics. Retrieved from https://stat.bora.dopa.go.th/stat/statnew/statMONTH/statmonth/#/mainpage

Centers for Disease Control and Prevention (CDC). (2024). Signs and symptoms of flu. Retrieved from https://www.cdc.gov/flu/signs-symptoms/index.html

Coddington, E. A., & Levinson, N. (1955). *Theory of ordinary differential equations*. New York, NY: McGraw-Hill.

Coleman, B. L., Fadel, S. A., Fitzpatrick, T., & Thomas, S-M. (2018). Risk factors for serious outcomes associated with influenza illness in high- versus low- and middle-income countries: Systematic literature review and meta-analysis. *Influenza and Other Respiratory Viruses*, *12*, 22-29. doi:10.1111/irv.12504

Department of Disease Control (DDC). (2024). Report on the seasonal influenza vaccination service, 2024. Retrieved from https://ddc.moph.go.th/uploads/publish/ 1693320250324062140.pdf

Diekmann, O., Heesterbeek, J. A. P., & Metz, J. A. J. (1990). On the definition and the computation of the basic reproduction ratio R_0 in models for infectious diseases in heterogeneous populations. *Journal of Mathematical Biology*, *28*, 365-382. doi:10.1007/BF00178324

Division of Epidemiology. (2025). Influenza surveillance report in Thailand, 2024: Week 51 (22th December - 28th December 2024). Retrieved from https://ddc.moph.go.th/uploads/ckeditor2/files/DOE_flu_51.2567.pdf

Froese, H., & Prempeh, A. G. A. (2022). Mask use to curtail influenza in a post–COVID-19 world: Modeling study. *JMIRx Med*, *3*(2), e31955. doi:10.2196/31955

Furushima, D., Kawano, S., Ohno, Y., & Kakehashi, M. (2017). Estimation of the basic reproduction number of novel influenza A (H1N1) pdm09 in elementary schools using the SIR model. *The Open Nursing Journal*, *11*, 64-72. doi:10.2174/1874434601711010064

Ho, B., & Chao, K. (2020). On the influenza vaccination policy through mathematical modeling. *International Journal of Infectious Diseases*, *98*, 71-79. doi:10.1016/j.ijid.2020.06.043

Imran, M., McKinney, B., & Butt, A. I. K. (2025). SEIR mathematical model for influenza-corona co-infection with treatment and hospitalization compartments and optimal control strategies. *Computer Modeling in Engineering & Sciences*, *142*(2), 1899-1931. doi:10.32604/cmes.2024.059552

Jan, J. (2024). How does the flu spread? All about flu transmission, contagious period, and more. Retrieved from https://www.goodrx.com/conditions/flu/is-the-flu-airborne

Jia, J., & Xiao, J. (2018). Stability analysis of a disease resistance SEIRS model with nonlinear incidence rate. *Advances in Difference Equations*, *2018*, 75. doi:10.1186/s13662-018-1494-1

Jonnalagadda, J. M. (2022). Epidemic analysis and mathematical modelling of H1N1 (A) with

vaccination. *Nonautonomous Dynamical Systems*, *9*(1), 1–10. doi: 10.1515/msds-2020-0143

Laguzet, L., & Turinici, G. (2015). Individual vaccination as Nash equilibrium in a SIR model with application to the 2009–2010 Influenza A (H1N1) epidemic in France. *Society for Mathematical Biology*, *77*, 1955-1984. doi:10.1007/s11538-015-0111-7

Leowattana, P., Luvira, V., Tangpukdee, N., Looareesuwan, P., Siripoon, T., Ngamprasertchai, T., . . . Chanthavanich, P. (2025). Knowledge, attitudes, practices and vaccine acceptance towards seasonal influenza vaccination among international travelers: A cross-sectional survey in Thailand. *Travel Medicine and Infectious Disease*, *66*, 102863. doi: 10.1016/j.tmaid.2025.102863

Maharany, & Mardiningsih. (2022). Stability analysis of equality point mathematics model of influenza virus in the human body with herbal treatment therapy. *Journal of Mathematics Education and Science*, *8*(1), 135-141.

Mohammad, K. M., & Kamrujjaman, M. (2024). Stochastic differential equations to model influenza transmission with continuous and discrete-time Markov chains. *Alexandria Engineering Journal*, *110*, 329-345. doi:10.1016/j.aej.2024.10.012

Safan, M. (2019). Mathematical analysis of an SIR respiratory infection model with sex and gender disparity: special reference to influenza A. *Mathematical Biosciences and Engineering*, *16*(4), 2613-2649. doi:10.3934/mbe.2019131

Seladi-Schulman, J. (2023). Flu facts: Incubation period and when it's contagious. Retrieved from https://www.healthline.com/health/flu-incubation-period

Tan, X., Yuan, L., Zhou, J., Zheng, Y., & Yang, F. (2013). Modeling the initial transmission dynamics of influenza A H1N1 in Guangdong Province, China. *International Journal of Infectious Diseases*, *17*, e479-e484.

Van Den Driessche, P., & Watmough, J. (2002). Reproduction numbers and sub-threshold endemic equilibria for compartmental models of disease transmission. *Mathematical Biosciences*, *180*, 29-48.

Viriyapong, R. (2021). *Introduction to mathematical modeling with differential equations*. Mueang, Phitsanulok: Naresuan University Publishing House.

World Health Organization. (2025). Influenza (Seasonal). Retrieved from https://www.who.int/news-room/fact-sheets/detail/influenza-(seasonal)

Wu, J. T., & Cowling, B. J. (2011). The use of mathematical models to inform influenza pandemic preparedness and response. *Experimental Biology and Medicine*, *236*(8), 955-961. doi:10.1258/ebm.2010.010271

Appendix

Appendix A

By substituting the dimensionless variables $\bar{S} = \frac{S}{N}$, $\bar{E} = \frac{E}{N}$, $\bar{I} = \frac{I}{N}$, and $\bar{R} = \frac{R}{N}$ into each equation of the system (1), then the equation dS/dt becomes

$$\begin{aligned}
\frac{dS}{dt} = \frac{d(\bar{S}N)}{dt} &= \alpha N - \frac{(1-\phi)\beta SI}{N} + \nu R - \mu S - \delta S, \\
\bar{S}\frac{dN}{dt} + N\frac{d\bar{S}}{dt} &= \alpha N - \frac{(1-\phi)\beta \bar{S}N\bar{I}N}{N} + \nu \bar{R}N - \mu \bar{S}N - \delta \bar{S}N, \\
\bar{S}(\alpha-\mu)N + N\frac{d\bar{S}}{dt} &= \alpha N - (1-\phi)\beta \bar{S}N\bar{I} + \nu \bar{R}N - \mu \bar{S}N - \delta \bar{S}N, \\
\bar{S}(\alpha-\mu) + \frac{d\bar{S}}{dt} &= \alpha - (1-\phi)\beta \bar{S}\bar{I} + \nu \bar{R} - \mu \bar{S} - \delta \bar{S}, \\
\frac{d\bar{S}}{dt} &= \alpha - (1-\phi)\beta \bar{S}\bar{I} + \nu \bar{R} - \mu \bar{S} - \delta \bar{S} - \bar{S}(\alpha-\mu), \\
\frac{d\bar{S}}{dt} &= \alpha - (1-\phi)\beta \bar{S}\bar{I} + \nu \bar{R} - \alpha \bar{S} - \delta \bar{S}.
\end{aligned}$$

Next, the equation dE/dt simplifies to

$$\begin{aligned}
\frac{dE}{dt} = \frac{d(\bar{E}N)}{dt} &= \frac{(1-\phi)\beta SI}{N} - \gamma E - \mu E, \\
\bar{E}\frac{dN}{dt} + N\frac{d\bar{E}}{dt} &= \frac{(1-\phi)\beta \bar{S}N\bar{I}N}{N} - \gamma \bar{E}N - \mu \bar{E}N, \\
\bar{E}(\alpha-\mu)N + N\frac{d\bar{E}}{dt} &= (1-\phi)\beta \bar{S}N\bar{I} - \gamma \bar{E}N - \mu \bar{E}N, \\
\bar{E}(\alpha-\mu) + \frac{d\bar{E}}{dt} &= (1-\phi)\beta \bar{S}\bar{I} - \gamma \bar{E} - \mu \bar{E}, \\
\frac{d\bar{E}}{dt} &= (1-\phi)\beta \bar{S}\bar{I} - \gamma \bar{E} - \mu \bar{E} - \bar{E}(\alpha-\mu), \\
\frac{d\bar{E}}{dt} &= (1-\phi)\beta \bar{S}\bar{I} - \gamma \bar{E} - \alpha \bar{E}.
\end{aligned}$$

Then, the equation dI/dt can be rewritten as

$$\begin{aligned}
\frac{dI}{dt} = \frac{d(\bar{I}N)}{dt} &= \gamma E - \sigma I - \mu I, \\
\bar{I}\frac{dN}{dt} + N\frac{d\bar{I}}{dt} &= \gamma \bar{E}N - \sigma \bar{I}N - \mu \bar{I}N, \\
\bar{I}(\alpha - \mu)N + N\frac{d\bar{I}}{dt} &= \gamma \bar{E}N - \sigma \bar{I}N - \mu \bar{I}N, \\
\bar{I}(\alpha - \mu) + \frac{d\bar{I}}{dt} &= \gamma \bar{E} - \sigma \bar{I} - \mu \bar{I}, \\
\frac{d\bar{I}}{dt} &= \gamma \bar{E} - \sigma \bar{I} - \mu \bar{I} - \bar{I}(\alpha - \mu), \\
\frac{d\bar{I}}{dt} &= \gamma \bar{E} - \sigma \bar{I} - \alpha \bar{I}.
\end{aligned}$$

And the equation dR/dt is expressed as

$$\begin{aligned}
\frac{dR}{dt} = \frac{d(\bar{R}N)}{dt} &= \sigma I - \nu R + \delta S - \mu R, \\
\bar{R}\frac{dN}{dt} + N\frac{d\bar{R}}{dt} &= \sigma \bar{I}N - \nu \bar{R}N + \delta \bar{S}N - \mu \bar{R}N, \\
\bar{R}(\alpha - \mu)N + N\frac{d\bar{R}}{dt} &= \sigma \bar{I}N - \nu \bar{R}N + \delta \bar{S}N - \mu \bar{R}N, \\
\bar{R}(\alpha - \mu) + \frac{d\bar{R}}{dt} &= \sigma \bar{I} - \nu \bar{R} + \delta \bar{S} - \mu \bar{R}, \\
\frac{d\bar{R}}{dt} &= \sigma \bar{I} - \nu \bar{R} + \delta \bar{S} - \mu \bar{R} \ - \bar{R}(\alpha - \mu), \\
\frac{d\bar{R}}{dt} &= \sigma \bar{I} - \nu \bar{R} + \delta \bar{S} - \alpha \bar{R}.
\end{aligned}$$

Appendix B

This demonstrates that $AB > C$.

$$\begin{aligned}
AB &= [a_1 + a_2 + a_3 + a_4(R_0 - 1)][(a_1 + a_2)a_3 + (a_1 + a_2 + \nu)a_4(R_0 - 1)] \\
&= (a_1 + a_2 + a_3)(a_1 + a_2)a_3 + (a_1 + a_2 + a_3)(a_1 + a_2 + \nu)a_4(R_0 - 1) \\
&+ (a_1 + a_2)a_3a_4(R_0 - 1) + (a_1 + a_2 + \nu)a_4^2(R_0 - 1)^2 \\
&> (a_1 + a_2 + a_3)(a_1 + a_2 + \nu)a_4(R_0 - 1) \\
&= (a_1^2 + a_2^2 + 2a_1a_2 + a_1a_3 + a_2a_3 + a_1\nu + a_2\nu + a_3\nu)\tfrac{a_1a_2a_3}{a_1a_2 + a_2\nu + \gamma\nu}(R_0 - 1) \\
&> (a_1a_2 + a_2\nu + a_1a_3)\tfrac{a_1a_2a_3}{a_1a_2 + a_2\nu + \gamma\nu}(R_0 - 1) \\
&= \big(a_1a_2 + a_2\nu + (\gamma + \alpha)(\nu + \alpha + \delta)\big)\tfrac{a_1a_2a_3}{a_1a_2 + a_2\nu + \gamma\nu}(R_0 - 1) \\
&= (a_1a_2 + a_2\nu + \gamma\nu + \gamma\alpha + \gamma\delta + \alpha\nu + \alpha^2 + \alpha\delta)\tfrac{a_1a_2a_3}{a_1a_2 + a_2\nu + \gamma\nu}(R_0 - 1) \\
&> (a_1a_2 + a_2\nu + \gamma\nu)\tfrac{a_1a_2a_3}{a_1a_2 + a_2\nu + \gamma\nu}(R_0 - 1) \\
&= a_1a_2a_3(R_0 - 1) \\
&= C
\end{aligned}$$